Science in China Series D: Earth Sciences

www.scichina.com
earth.scichina.com
www.springerlink.com

Ensemble prediction experiments using conditional nonlinear optimal perturbation

JIANG ZhiNa[1,2†], MU Mu[2] & WANG DongHai[1]

[1] State Key Laboratory of Severe Weather (LaSW), Chinese Academy of Meteorological Sciences, Beijing 100081, China;
[2] State Key Laboratory of Numerical Modeling for Atmospheric Sciences and Geophysical Fluid Dynamics (LASG), Institute of Atmospheric Physics, Chinese Academy of Sciences, Beijing 100029, China

Two methods for initialization of ensemble forecasts are compared, namely, singular vector (SV) and conditional nonlinear optimal perturbation (CNOP). The comparison is done for forecast lengths of up to 10 days with a three-level quasi-geostrophic (QG) atmospheric model in a perfect model scenario. Ten cases are randomly selected from 1982/1983 winter to 1993/1994 winter (from December to the following February). Anomaly correlation coefficient (ACC) is adopted as a tool to measure the quality of the predicted ensembles on the Northern Hemisphere 500 hPa geopotential height. The results show that the forecast quality of ensemble samples in which the first SV is replaced by CNOP is higher than that of samples composed of only SVs in the medium range, based on the occurrence of weather regime transitions in Northern Hemisphere after about four days. Besides, the reliability of ensemble forecasts is evaluated by the Rank Histograms. The above conclusions confirm and extend those reached earlier by the authors, which stated that the introduction of CNOP improves the forecast skill under the condition that the analysis error belongs to a kind of fast-growing error by using a barotropic QG model.

ensemble prediction, medium range, singular vector, conditional nonlinear optimal perturbation

The atmosphere is a complicated nonlinear system, and even an infinitesimally small perturbation introduced into the state of the atmosphere at a given time will result in an increasingly great change in the evolution of the atmosphere with time, so that after about two or three weeks the trajectories of the perturbed and the original atmosphere would be completely different. This is the atmospheric chaotic nature[1]. For very short range, the forecast can be considered deterministic, but as forecast time advances, one cannot ignore the reality of a range of plausible outcomes. Then, weather prediction becomes a kind of probability estimate of the future weather conditions.

A computationally tractable method to approximate the evolution of the probability density function is through ensemble forecasting. Epstein[2] and Leith[3] opened the door for ensemble prediction. In adopting the ensemble approach, one explicitly recognizes that forecasts, especially for the medium range (and beyond), should be considered stochastic, not deterministic, in nature. There is no single valid solution but rather a range of possible solutions[4]. One of the key problems in ensemble prediction is the generation of initial ensemble perturbations, namely, how to generate the initial perturbations that can reflect the real initial uncertainty.

Monte Carlo method was first applied to ensemble prediction by Leith[3], which is based on their interpretation as a random sample of a probability distribution. In recent year, it has become apparent that this method is not the best way of making ensemble forecasts. This is because random errors in the analysis field belong to

Received July 25, 2008; accepted September 11, 2008; published online February 26, 2009
doi: 10.1007/s11430-009-0042-y
†Corresponding author (email: jzn@cams.cma.gov.cn)
Supported by Knowledge Innovation Project of the Chinese Academy of Sciences (Grant No. KZCX3-SW-230), National Natural Science Foundation of China (Grant Nos. 40675030, 40633016)

slow-growing or non-growing type of errors. However, the growing type of errors in the analysis field, such as baroclinic instability[5], is much more important than the non-growing errors in determining the skill of any specific forecast. The difference between the analysis at a given initial time and a very-short-range forecast verifying at the same time can therefore be considered as a growing perturbation consistent with the uncertainty in the initial conditions. This idea is exploited in the lagged average forecasting (LAF) method proposed by Hoffman and Kalnay[6]. There are different confidences in the ensemble members, which makes the ensemble size limited. So, Ebisuzaki and Kalnay[7] proposed a scaled LAF method in which perturbations are considered equally likely. Gong et al.[8] proposed a new method of four dimensional variation to form a set of perturbations in line with the dynamical model, which has the advantages of both statistical significance of Monte Carlo and different initial values information of LAF.

After about twenty years, ensemble prediction went into operational implementation in the early 1990s. National Centers for Environmental Prediction (NCEP), European Centre for Medium-Range Weather Forecasts (ECMWF), and Meteorological Service of Canada (MSC) all developed their own ensemble prediction systems. Toth and Kalnay[9]extended Lyapunov exponents into the nonlinear domain to propose a new method called breeding of the growing vectors of the atmosphere, which is a kind of self-sustainable fast-growing perturbations. Assuming errors in the initial conditions are dominated by those instabilities of the flow that developed over a series of previous assimilation cycles, which is the basis of ensemble perturbations in NCEP[5]. A combination of total energy-based singular vectors (SVs) has been used to sample analysis uncertainty for initial ensemble perturbations at ECMWF[10]. The successful application of this method is based on the fact that SVs maximize growth over a finite time interval and are consequently expected to dominate forecast errors at the end of that interval and possibly beyond[11]. In recent years, the diabatic process is introduced to the tangent linear and adjoint models. Forecasts based on initial conditions perturbed by moist SVs show that the ensemble forecast skill on the path and intensity of extratropic cyclones have been improved[12]. At MSC a 'perturbed-observation' statistical interpolation is used[13]. These three methods have been compared in a series of papers[14−16], and certainly, each has its own merits.

Singular Vectors are the fastest growing perturbations in the early forecast, which determine the unstable directions in the linear range. However, Gilmour and Smith[17] presented that there are limits of linearity assumptions in the construction of ensemble perturbation. Given that the singular vectors cannot capture the nonlinear characteristics, a new concept of conditional nonlinear optimal perturbation was proposed[18], which is a natural extension of SV into the nonlinear regime. In our earlier studies, by using a barotropic QG model, it was shown that when the analysis error is a kind of fast-growing error, the forecast skill of ensemble samples in which the first SV is replaced by CNOP is comparatively higher than that of samples composed of only SVs in the medium range. More experiments further illustrate that the new method has made higher reliability than SV method by the analysis of spread-skill relations and Talagrand diagrams. Considering that the barotropic model used above cannot simulate the real large-scale circulation, then in this paper, we use the T21L3 QG model to further explore the application of CNOP to ensemble prediction, emphasizing what kind of initial errors CNOPs can represent well in the atmosphere so that the forecast skill of some specific weather events can be improved. A 'perfect model' scenario is used so that all predictions errors are due to the uncertainty in the initial conditions.

1 The model, methods and experimental setup

1.1 Model

The nonlinear model used in this study is the quasi-geostrophic global spectral model of Marshall and Molteni[19], with triangular truncation T21. It includes orography, and is driven by empirical forcing functions. The integrated variables are potential vorticity at 200, 500, and 800 hPa. The global model has been tuned to describe a perpetual winter situation in the Northern Hemisphere. Thanks to its ease of use, transparent coding, and realism, the model has been used in the fields of predictability and ensemble prediction[14,20−23].

1.2 SVs and CNOPs

For fixed $T > 0$ and initial potential vorticity $Q|_{t=0} = Q_0$, the propagator M is well-defined; $Q(T)=M_T(Q_0)$ is the solution of the nonlinear model at time T. The tangent linear propagator M and the corresponding adjoint version M^* are available.

Two kinds of norms are adopted in this study. The streamfunction squared norm is

$$\|q\|_{\mathrm{S}}^2=[q,q]_{\mathrm{S}}=\left\langle \mathrm{E}^{-1}q,\mathrm{E}^{-1}q\right\rangle=\frac{1}{V}\int_V(\mathrm{E}^{-1}q)(\mathrm{E}^{-1}q)\mathrm{d}V, \tag{1}$$

and total energy norm is

$$\|q\|_{\mathrm{TE}}^2=(q,q)_{\mathrm{TE}}=\left\langle q,-\mathrm{E}^{-1}q\right\rangle=-\frac{1}{V}\int_V\left(q(\mathrm{E}^{-1}q)\right)\mathrm{d}V, \tag{2}$$

which are all integrated over the whole atmosphere V, where q is the potential vorticity perturbation. Defining q=Eφ with the streamfunction perturbation φ, where E is the linear operator that transforms streamfunction into potential vorticity, and E^{-1} is the inverse operator, which transforms potential vorticity into streamfunction.

Conditional nonlinear optimal perturbation (CNOP) is defined as such a kind of initial perturbation $q_{0\sigma}^*$, which makes the objective function $J(q_0)$ acquire the maximum under the initial constraint condition $\|q_0\|_{\mathrm{S}}\leqslant\sigma$,

$$J(q_{0\sigma}^*)=\max_{\|q_0\|_{\mathrm{S}}\leqslant\sigma}J(q_0), \tag{3}$$

where

$$J(q_0)=\left\|M_T(Q_0+q_0)-M_T(Q_0)\right\|_{TE}. \tag{4}$$

Q_0 and q_0 represent initial basic state and perturbation respectively, and σ is a presumed positive constant representing the magnitude of the initial uncertainty.

To capture the maximum of $J(q_0)$ with the constraint $\|q_0\|_S\leqslant\sigma$, we calculate the minimum of another new objective function $J_1(q_0)$ with $\|q_0\|_S\leqslant\sigma$. The new objective function is defined as

$$J_1(q_0)=-[J(q_0)]^2=-\left\|M_T(Q_0+q_0)-M_T(Q_0)\right\|_{TE}^2. \tag{5}$$

The first variation of $J_1(q_0)$ is

$$\begin{aligned}\delta J_1(q_0)=&-(2\mathrm{M}^{\mathrm{TE}*}(Q_0+q_0)[M_T(Q_0+q_0)\\&-M_T(Q_0)],\delta q_0)_{\mathrm{TE}}.\end{aligned} \tag{6}$$

According to Buizza et al.[24], the adjoint operator M^{TE*} with respect to the above total energy norm can be deduced from M^*. Here, $\mathrm{M}^{\mathrm{TE}*}=\mathrm{EM}^*\mathrm{E}^{-1}$. Then,

$$\begin{aligned}\delta J_1(q_0)=&-(2\mathrm{EM}^*(Q_0+q_0)\mathrm{E}^{-1}[M_T(Q_0+q_0)\\&-M_T(Q_0)],\delta q_0)_{\mathrm{TE}}\\=&(\nabla J_1,\delta q_0)_{TE}.\end{aligned} \tag{7}$$

Optimization algorithm of spectral projected gradient 2 (SPG2) Method[25] is employed in this research, which calculates the least value of a function of several variables subject to box and ball constraints. To use the SPG2 method, subroutines which evaluate the objective function and its gradient need to be supplied by the user. The above deduction has provided these conditions. According to the definition of CNOP, CNOP is the global maximum of the cost function. However, there exists the possibility that the cost function attains its local maximum in a small neighborhood of a point in the phase space. Such an initial perturbation is called local CNOP. Singular vectors are computed by an iterative power method. The total energy norm is also chosen in this process. The detailed procedure can be found in Farrell and Moore[26].

1.3 Experimental setup

This study is carried out under a perfect model scenario. First, the nonlinear model is used to produce a reference atmospheric state starting from specified ECMWF operational analysis streamfunction data, which are randomly selected from 1982/1983 winter to 1993/1994 winter (from December to the following February). This state is regarded as a 'true' state with which all predictions will be compared. The state of control forecast is then produced with the same model starting from the initial control run state, whose generation will be described in section 3.1. Both SVs and CNOPs are calculated by using the state of control forecast as basic state with optimization time of two days. SVs are scaled to have the same initial constraint condition with CNOP, whose amplitude is within the initial control run error. Then, the directions of the initial ensemble perturbations are constructed as a simple random linear combination of the above two kinds of initial perturbations,

$$pert_j=\sum_i\alpha_{ij}v_i\Big/\sum_i\alpha_{ij}, \tag{8}$$

where α_{ij} are independent variables of the Gaussian distribution N(0,1); i=1, 2, 3; j=1, 2, 3. v_1 represents the first SV or CNOP. v_2 represents the second SV. v_3 represents the third SV. Such perturbations $pert_j$, together with their opposites $-pert_j$, are added to the initial control state to generate the perturbed initial fields. One ensemble sample is composed of perturbed forecasts and one control forecast. Thus, seven ensemble members are generated. If the first SV represents v_1, ensemble sample is denoted as S1. If the global CNOP represents v_1, ensemble sample is denoted as S2. For S3, local CNOP represents v_1. The forecast length is up to 10 days.

2 Numerical results

2.1 Generation of initial control state

We performed a three-dimensional variation data assimilation to generate the initial control state. First, at each grid point, observation is generated by adding a random error with normal distributions $N(0, R)$ to the true value. The observation covariance matrix R, taken from Houtekamer and Mitchell[21], includes correlation among the three model levels, but no horizontal correlation. The background field is acquired through integrating the nonlinear model from ECMWF operational analysis streamfunction data ahead 12 hours of the true initial state. Then we define the following objective function

$$J_2(\psi_0^*) = \min_{\psi_0} J_2(\psi_0), \tag{9}$$

where

$$J_2(\psi_0) = \frac{1}{2}(\psi_0 - \psi_0^b)^{\mathrm{T}} B^{-1}(\psi_0 - \psi_0^b) + \frac{1}{2}(\psi_0 - \psi_0^{\mathrm{obs}})^{\mathrm{T}} R^{-1}(\psi_0 - \psi_0^{\mathrm{obs}}), \tag{10}$$

where T represents the matrix transpose, B^{-1} and R^{-1} represent the inverse of the covariance matrix of the background error and observational error respectively, which are both assumed diagonal. ψ_0^{obs} represents the observation field at T_0, and ψ_0^b background field at T_0. ψ_0^* is the optimal initial field at which the objective function attains the minimum, and is adopted as the initial control state.

2.2 Forecast experiments

In the following, we present a series of experiments, each of which corresponds to a different truth run. The evaluation is made on the Northern Hemisphere 500 hPa geopotential height. Anomaly correlation coefficient (ACC) is adopted as a tool to measure the quality of the predicted ensembles. The climatological state is obtained through 20 years (corresponding to 1800 days) integrations from ECMWF operational analysis of 00 UTC 1 December 1983. Table 1 concludes 10 cases including the beginning time, the root mean squared errors on the Northern Hemisphere 500 hPa geopotential height, the days for ACC⩾0.6 for control run and other ensemble forecasts, and whether S2/S3 improves the forecast skill compared with S1 or not. For each case, the evolutions of ACC of ensemble S1, S2 and S3 are calculated respectively. Little difference is found in the early days among them, so we only pay attention to the magnitude of ACC after three days. If after 3 days the ACC value of S2/S3 is larger than that of S1 all along, we define that S2/S3 improves the forecast skill. Whereas, we define S2/S3 does not improve the forecast skill. ‘ √ ’represents S2/S3 improves the forecast skill on the whole; ‘×’on the contrary. Especially, for case 2, S2/S3 improves the forecast skill only in the later part of the forecast. While for case 3, S2/S3 improves the forecast skill only in the earlier part of the forecast.

Table 1 shows that in some cases the introduction of CNOP can improve the forecast skill, whereas, in other cases, it may make the forecasts bad. In conclusion, for the cases in which the introduction of CNOP makes the forecasts bad, the days for ACC⩾0.6 for control run are longer. In other words, the control run can provide a good forecast, and the atmospheric predictability is comparatively high. However, if the atmospheric predictability is comparatively low, the introduction of CNOP can improve the forecast skill. Certainly, there is great difficulty to make the days for ACC⩾0.6 of S2/S3 longer than those of S1 at least one day, even though the new ensemble perturbation method can improve the forecast skill. Furthermore, it is found that the forecast skill is not entirely dependent on the magnitude of initial errors. Hence, we raise the question: what determines the atmospheric predictability besides the magnitude of the initial errors? In the following, we analyze the evolution of the general circulations to obtain some information.

2.3 General circulation analysis

For the above 10 control runs, the days for ACC⩾0.6 are all over 5 days, so we focus on the evolution of the general circulation at 500 hPa after 4 days. In conclusion, it is found that except cases 6, 9, 10, the introduction of CNOP improves the forecast skill on the whole. Moreover, in the residual cases, except case 2, there appear weather regime transitions. There are blockings appearing over European area for cases 1, 3, 7; and there are blockings appearing over East Pacific-North American area for cases 4, 5, 8.

As an example of case 8, Figure 1 presents the evolution of the true streamfunction field on Northern Hemisphere 500 hPa. It is shown that for the true state, there persists a zonal flow on the Northern Hemisphere 500 hPa before day 6. Afterwards, a blocking occurs over north Pacific area, which persists until day 10. For the

Table 1 Results for 10 experiments

Case	Beginning time	Magnitude of analysis error (gpm)	Control (day)	S1 (day)	S2 (day)	S3 (day)	S2/S3 improve forecast skill or not
1	1986-01-20	7.1	5	5	6	6	√
2	1987-01-18	40.6	5	6	6	6	× √
3	1989-02-02	29.1	6	8	8	8	√ ×
4	1990-01-28	35.0	6	7	7	8	√
5	1991-01-12	32.6	6	8	8	\	√
6	1992-02-08	10.5	9	9	9	9	×
7	1992-12-02	20.1	6	8	8	8	√
8	1992-12-07	24.0	6	8	8	8	√
9	1993-01-05	3.8	10	10	10	10	×
10	1993-01-20	36.7	10	10	10	10	×

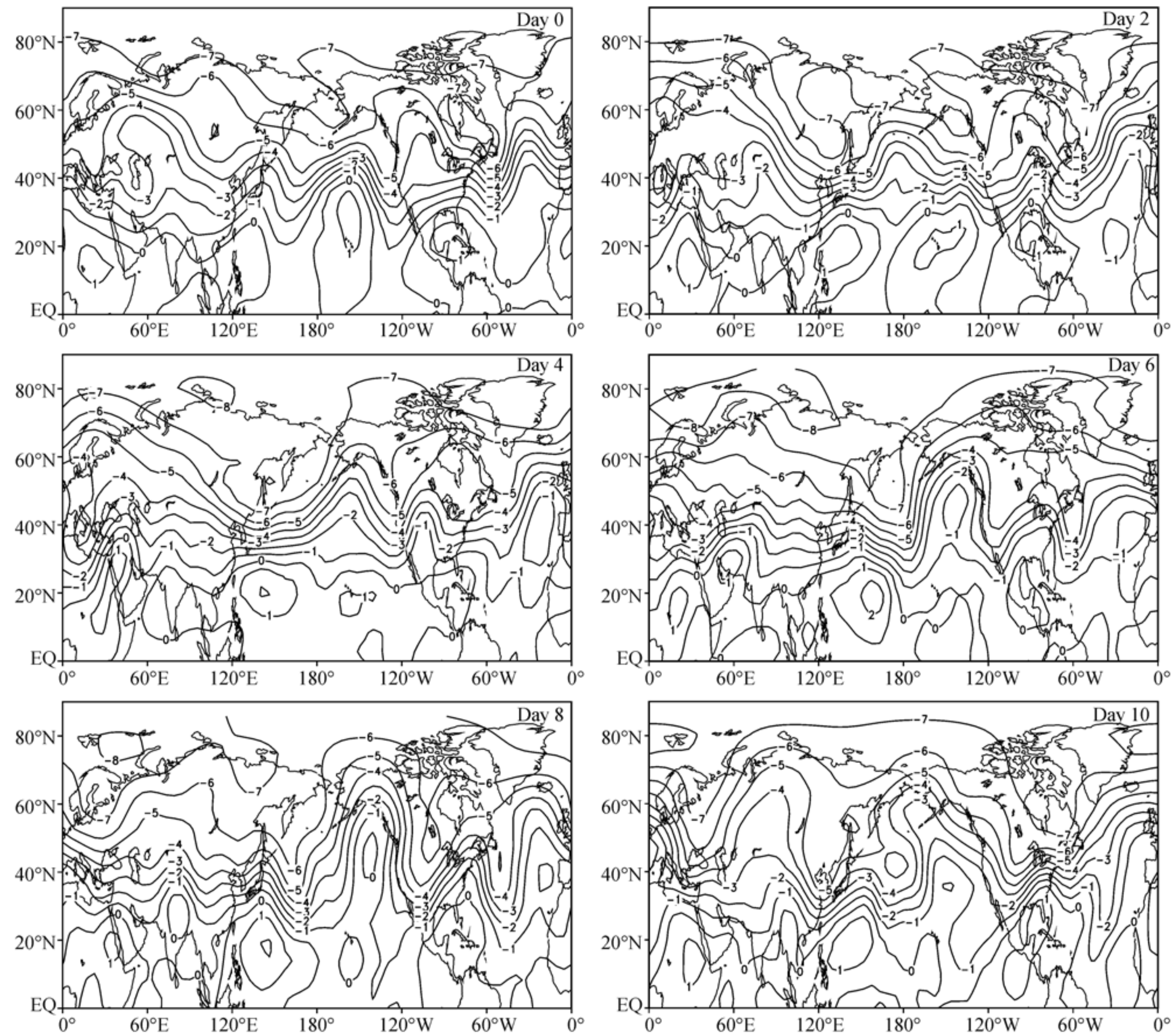

Figure 1 Evolution of the true streamfunction field on Northern Hemisphere 500 hPa, as an example of case 8 (10^7 $m^2 \cdot s^{-1}$).

control run, there is a zonal flow before day 6. The value of ACC for the first 6 days is not less than 0.6, and then the forecast before day 6 can be considered valid. Though a blocking occurred over north Pacific area at day 6, it is very weak and at day 10 it disappeared (not shown). In other words, for this case the control run cannot capture such a weather regime transition so that the control forecast skill is lower in the later forecast range. However, the introduction of CNOP makes ensemble perturbations capture the fast-growing analysis error and then improves the forecast quality.

Similarly, we analyzed cases 6, 9 and 10 in which the introduction of CNOP makes the forecasts bad. It is found that for all three cases, there persist zonal flows on Northern Hemisphere 500 hPa in the medium range. As an example of case 10, Figure 2 shows the time evolution of the true streamfunction field on Northern Hemisphere 500 hPa. It is seen that there is a weak blocking over East Asia-north west Pacific area before day 4. Though there appears weather regime transition from blocking to zonal flow, it happens in the earlier part of the forecast when the control run can provide a better forecast skill. Afterward, there persists zonal flow on Northern Hemisphere for the true state. Moreover, for the control run, in the whole forecast period the control run has provided a very good forecast. In other words, the atmospheric predictability is comparatively high if there is no weather regime transition in the medium range.

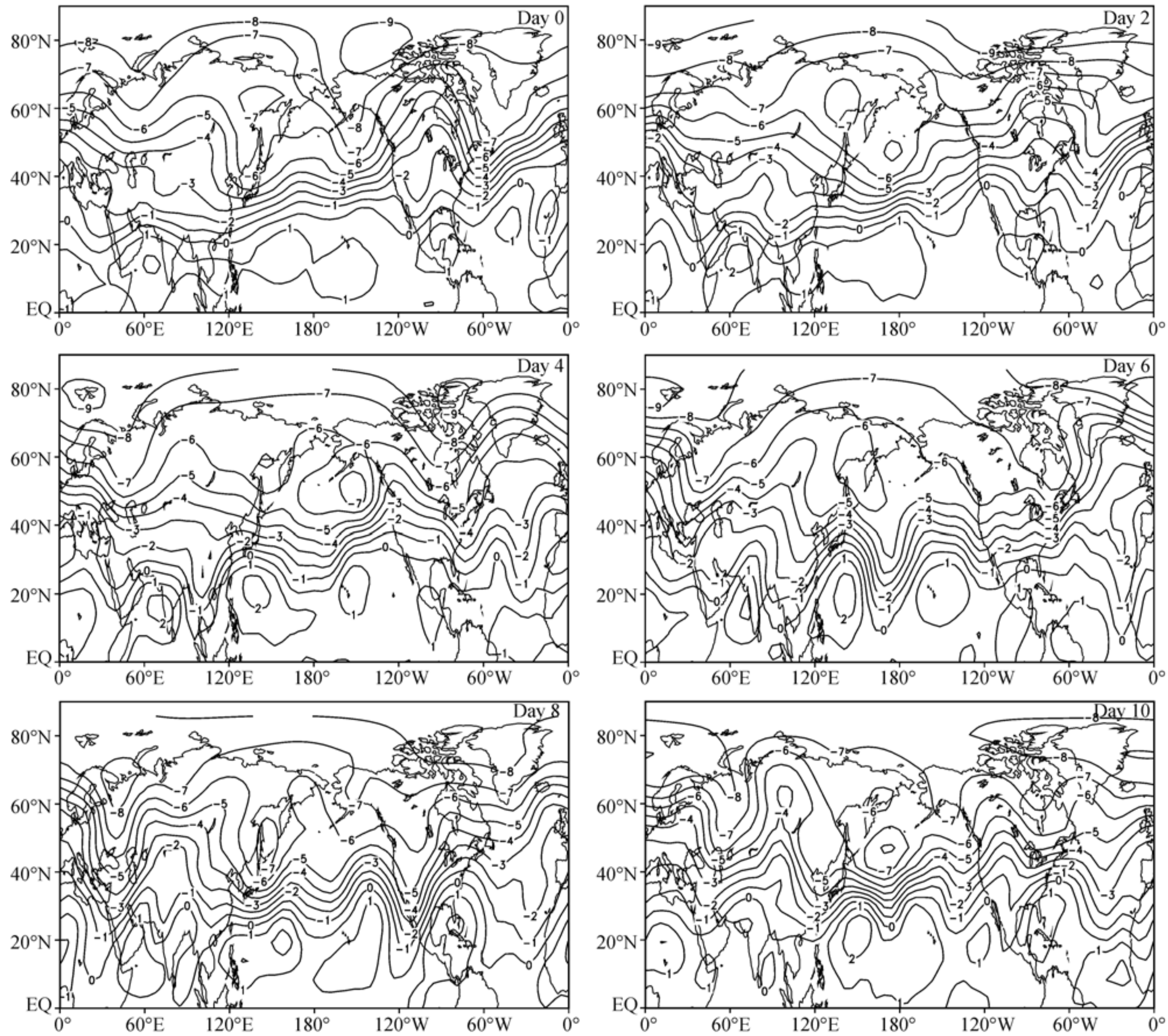

Figure 2 Evolution of the true streamfunction field on Northern Hemisphere 500 hPa, as an example of case 10 (10^7 $m^2 \cdot s^{-1}$).

From the above analysis, we found that if a large-scale weather regime transition occurs in the real atmosphere in the medium range, it is difficult for a single deterministic forecast to capture such a phenomenon, while the introduction of CNOP can improve the forecast skill. Molteni and Palmer[20] pointed out that weather regime transition usually is related to fast-growing errors. Similarly, in the earlier work by Mu and Jiang[27], it is shown that under the condition that the analysis error is a kind of fast-growing error, the introduction of CNOP can improve the forecast skill by using a barotropic QG model. This suggests that our conclusion is consistent with their results[27].

3 Validation

As a first measure of the forecast quality of the predicted ensemble, Figure 3 shows the time evolution of ACC of the ensemble mean for the cases in which the introduction of CNOP (partly) improves the forecast skill. It is seen that, from about day 4 to 8, the skill of the ensemble mean is clearly higher for the local CNOP, then the global CNOP, and finally the SV method. The days for ACC⩾0.6 for ensemble prediction are at least one day longer than those for the control run.

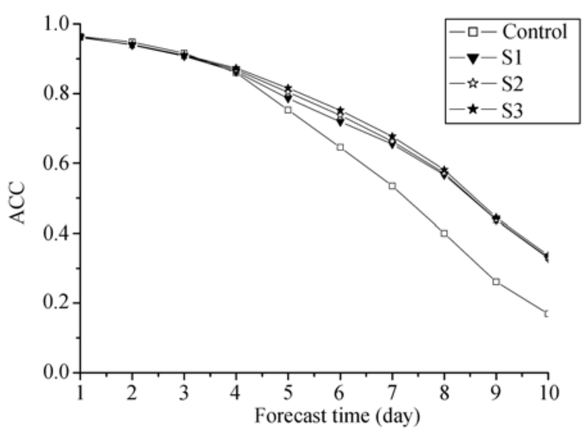

Figure 3 Evolution of ACC of the ensemble mean forecast as a function of lead time.

Then, the Rank Histograms, also known as Talagrand diagrams, are adopted as a tool for evaluating the reliability of ensemble forecasts[28]. It must be statistically flat for a perfectly reliable prediction system. However, exact flatness cannot be expected because of the finiteness of the number M of realizations of the prediction process. The deviation from flatness of the histogram can be measured by

$$\Delta = \frac{1}{m}\sum_{k=1}^{N+1}\left(S_k - \frac{m}{N+1}\right)^2, \tag{11}$$

where S_k is the number of elements in the kth interval of the histogram. From a perfectly reliable system, Δ is on average equal to $\Delta_0=N/(N+1)$. Following Candille and Talagrand[29], the ratio

$$\delta = \frac{\Delta}{\Delta_0} \tag{12}$$

as a measure of the effective flatness of the histogram. The smaller the score δ is, the more reliable the ensemble forecast is.

Figure 4 presents the temporal variation of the score δ of the rank histogram for the cases in which the introduction of CNOP improves the forecast skill. Both the SV and CNOP methods have large initial scores, which decrease significantly in the course of the forecast. The introduction of local CNOP clearly has the best performance in the medium range. And global CNOP has the best performance in the earlier part. The above numerical experiments indicate that the role of local CNOP in the construction of ensemble perturbations may not be omitted.

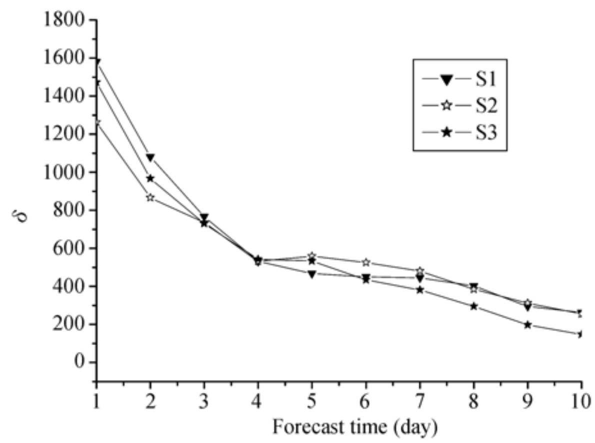

Figure 4 Evolution of the normalized score δ of the rank histogram as a function of lead time.

4 Conclusions and discussion

In this paper, a T21L3 quasi-geostrophic model is used to perform the ensemble prediction experiments. All our tests are based on a perfect model scenario, so all prediction errors are caused by those in the initial state. A systematic comparison has been performed of the SV and CNOP methods for initialization of ensemble prediction. The general conclusion is that when there is blocking onset for Northern Hemisphere in the medium range forecast, the introduction of CNOP, especially the local CNOP, provides a better performance for the forecast quality, which is measured by Anomaly correlation coefficient. The Rank Histograms show that the role of local CNOP in the construction of ensemble perturbations may not be neglected. The results confirm and extend those obtained by Mu and Jiang[27].

Admittedly, our experiments are based on a perfect model scenario, whereas, the assumption is not a realistic analog for actual numerical weather prediction, where model error may be significant or even dominant. Therefore, the application of CNOP to operational ensemble prediction system still has a long way to go, which needs to be explored. Besides, our results show that if there is a weather regime transition, the introduction of CNOP could improve the forecast quality. Contrariwise, the introduction of CNOP may make the forecast bad. But for real atmospheric forecasting, no one can know in *a priori* whether there will be weather regime transition, and thus it is difficult for us to choose the method for generation of ensemble perturbations. Moreover, if the ensemble prediction using our method forecasts out some weather events which often do not happen in the real atmosphere, it is not acceptable to use our method to make the ensemble prediction. Considering that the ensemble prediction using the original method may not forecast out the weather events which do happen in the real atmosphere, as a more immediate goal, it is necessary to distinguish the two contrary situations to seek how to combine the various methods to make the ensemble perturbations. It is expected that further study on applications of nonlinear optimization technique to ensemble prediction may offer guidelines for the future development of ensemble forecasting technique.

We thank the three anonymous reviewers for their valuable suggestions for improvement of this manuscript.

1 Lorenz E N. Deterministic nonperiodic flow. J Atmos Sci, 1963, 20: 130－141
2 Epstein E S. Stochastic dynamic prediction. Tellus, 1969, 21: 739－759
3 Leith C E. Theoretical skill of Monte Carlo forecasts. Mon Weather Rev, 1974, 102: 409－418
4 Tracton S M, Kalnay E. Operational ensemble prediction at the national meteorological center: Practical aspects. Weather Forecast, 1993, 8(3): 379－400
5 Toth Z, Kalnay E. Ensemble forecasting at NCEP and the breeding method. Mon Weather Rev, 1997, 125(12): 3297－3319
6 Hoffman R N, Kalnay E. Lagged average forecasting, an alternative to Monte-Carlo forecasting. Tellus, 1983, 35: 100－118
7 Ebisuzaki W, Kalnay E. Ensemble experiments with a new lagged average forecasting scheme. WMO Report #15. 1991
8 Gong J D, Li W J, Chou J F. Forming proper ensemble forecast initial members with four dimensional variational data assimilation method (in Chinese). Chin Sci Bull, 1999, 44(10): 1113－1115
9 Toth Z, Kalnay E. Ensemble forecasting at NMC: The generation of perturbations. Bull Amer Meteorol Soc, 1993, 74(12): 2317－2330
10 Ehrendorfer M, Tribbia J J. Optimal prediction of forecast error covariances through singular vectors. J Atmos Sci, 1997, 54: 286－313
11 Molteni F, Buizza R, Palmer T N, et al. The new ECMWF Ensemble Prediction System: Methodology and validation. Q J R Meteorol Soc, 1996, 122: 73－119
12 Hoskins B J, Coutinho M M. Moist singular vectors and the predictability of some high impact European cyclones. Q J R Meteorol Soc, 2005, 131: 581－601
13 Houtekamer P L, Lefaivre L, Derome J, et al. A system simulation approach to ensemble prediction. Mon Weather Rev, 1996, 124(6): 1225－1242
14 Houtekamer P L, Derome J. Methods for ensemble prediction. Mon Weather Rev, 1995, 123(7): 2181－2196
15 Hamill T M, Snyder C, Morss R E. A comparison of probabilistic forecasts from bred, singular-vector, and perturbed observation ensembles. Mon Weather Rev, 2000, 128: 1835－1851
16 Buizza R, Houtekamer P L, Toth Z, et al. A comparison of the ECMWF, MSC, and NCEP global ensemble prediction systems. Mon Weather Rev, 2005, 133(5): 1076－1097
17 Gilmour I, Smith L A. Enlightenment in shadows. In: Kadtke J B, Bulsara A, eds. Applied Nonlinear Dynamics and Stochastic Systems near the Millennium. AIP Conference Proceedings, San Diego, July 1, 1997. 335－340
18 Mu M, Duan W S, Wang B. Conditional nonlinear optimal perturbation and its application. Nonlinear Proc Geoph, 2003, 10: 493－501
19 Marshall J, Molteni F. Toward a dynamical understanding of planetary-scale flow regimes. J Atmos Sci, 1993, 50: 1792－1818
20 Molteni F, Palmer T N. Predictability and finite-time instability of the northern winter circulation. Q J R Meteorol Soc, 1993, 119: 269－298
21 Houtekamer P L, Mitchell H L. Data assimilation using an ensemble kalman filter technique. Mon Weather Rev, 1998, 126: 796－811
22 Ehrendorfer M. The total energy norm in a quasigeostrophic model. J Atmos Sci, 2000, 57: 3443－3451
23 Descamps L, Talagrand O. On some aspects of the definition of initial conditions for ensemble prediction. Mon Weather Rev, 2007, 135: 3260－3272
24 Buizza R, Tribbia J, Molteni F, et al. Computation of optimal unstable structures for a numerical weather prediction model. Tellus, 1993, 45: 388－407
25 Birgin E G, Martinez J M, Raydan M. Nonmonotone spectral projected gradient methods for convex sets. SIAM J Opt, 2000, 10(4): 1196－1211
26 Farrell B F, Moore A M. An adjoint method for obtaining the most rapidly growing perturbation to oceanic flows. J Phys Oceanogr, 1992, 22: 338－349
27 Mu M, Jiang Z N. A new approach to the generation of initial perturbations for ensemble prediction: Conditional nonlinear optimal perturbation. Chin Sci Bull, 2008, 53(13): 2062－2068
28 Talagrand O, Vautard R, Strauss B. Evaluation of probabilistic prediction system. In: ECMWF Proceeding of Workshop on Predictability, 1999. 1－25
29 Candille G, Talagrand O. Evaluation of probabilistic prediction systems for a scalar variable. Q J R Meteorol Soc, 2005, 131: 2131－2150